Am J Cancer Res 2021;11(11):5581-5590
www.ajcr.us /ISSN:2156-6976/ajcr0137452

Original Article

MEK1/2 regulates APOBEC3B and polymerase iota-induced mutagenesis in head and neck cancer cells

Dominik Schulz[1], Guido Piontek[2], Ulrich M Zissler[3], Gabriele Multhoff[4], Markus Wirth[5], Anja Pickhard[5]

[1]Department of Internal Medicine II, Klinikum Rechts der Isar, Ismaninger Straße 22, Munich 81675, Germany; [2]Institute of Pathology, Ludwig Maximilians University of Munich, Munich 81377, Germany; [3]Center of Allergy & Environment (ZAUM), German Research Center for Environmental Health, Member of The German Center for Lung Research (DZL), Helmholtz Center Munich, Technical University of Munich (TUM), Biedersteiner Street 29, Munich 80333, Germany; [4]Department of Radiotherapy, Technical University of Munich, Ismaninger Straße 22, Munich 80333, Germany; [5]Department of Head and Neck Surgery, Klinikum Rechts der Isar, Ismaninger Straße 22, Munich 81675, Germany

Received July 17, 2021; Accepted September 9, 2021; Epub November 15, 2021; Published November 30, 2021

Abstract: Resistance to chemotherapy provides a major challenge in treatment of metastatic cancer. Prolonged exposure to almost any drug regimen leads to the formation of resistant subclones in almost all advanced solid tumors. Tumor heterogeneity because of intrinsic genetic instability is seen as one of the major contributing factors. In this work, we present evidence that genetic instability measured by mutation frequency is induced by treatment with the EGFR inhibitor afatinib or cisplatin in head and neck squamous cancer cells. We find that APOBEC3B and polymerase iota are upregulated, and inhibition of MEK1/2 by U0126 leads to downregulation on the protein level. Costimulation of afatnib and cisplatin with U0126 leads to a significantly lower mutation frequency. These findings may represent a molecular mechanism for dynamically controlling genetic instability during chemotherapy in head and neck squamous cell carcinoma (HNSCC) cancer cells.

Keywords: Hypermutation, mutagenesis, HNSCC, APOBEC3B, polymerase iota, MEK1/2

Introduction

Acquired chemoresistance severely limits the prognosis of disseminated malignancies. After initial response, most advanced tumors become resistant to therapy, and continuous treatment with the same regimen has little to no effect. Although mechanisms of drug resistance-such as increased efflux, reduced absorption, inhibition of cell death, and changes in tumor microenvironment and cancer stem cells have been identified-mechanisms of development of these cellular eviction strategies remain largely unknown.

It is commonly assumed that acquired chemoresistance is associated with the emergence of drug refractory subpopulations [1]. These are formed because of the inherent genetic instability, and they select as the fittest under chemotherapeutic treatment. Due to the random nature of mutations, this paradigm assumes the lack of directionality [2]. However, there is also evidence that exogenic stress could activate cellular pathways that promote genetic instability. In E. coli, stress-like starvation induces activation of the RNA polymerase, sigma S (RpoS) system, leading to error-prone double-strand break repair, potentially accelerating evolution [3].

In our previous work, we demonstrated that that long-term exposure of two HNSCC cell lines to five targeted therapies and chemotherapeutics leads to an eightfold increase in mutation rate compared to untreated cells [4]. In this study, we present therapy-induced APOBEC3B (A3B) and polymerase iota (Pol i) activation as a possible mechanism for the observed hypermutation.

Materials and methods

Cell culture and reagents

We obtained University of Düsseldorf squamous cell carcinoma-5 (UD-SCC-5) cells from the university's Clinic for Otolaryngology, Düs-

seldorf, Germany. We used Dulbecco's modified Eagle medium (DMEM; Invitrogen, Darmstadt, Germany) with 10% fetal calf serum (FBS; Biochrom, Berlin, Germany), 2 mM glutamine (Biochrom), 100 µg/ml streptomycin (Biochrom), and 100 U/ml penicillin (Biochrom) to culture the cells. Cells were cultivated at 37°C with 5% CO_2, and grown a confluence of 75-85%. The EGFR inhibitor afatinib (Selleckchem, Houston, TX) and chemotherapeutic cisplatin (Selleckchem, Houston, TX) were used.

UD-SCC-5 cells were treated with 2xIC_{50} for 24 hours or 168 hours without changing the medium (IC_{50} afatinib 2.24 nM, cisplatin 1.96 µM; [4]. Furthermore, we used previously generated afatinib- and cisplatin-resistant clones (AfaRes and CisRes; [4].

RNA isolation and whole genome microarray

For extracting the total RNA we used the RNeasy Mini Kit (Qiagen). To avoid DNA contamination we used on-column DNase digestion (Qiagen). RNA quantification and quality assessments were performed with the help of ultraviolet-visible spectrophotometry (Nanodrop Technologies, Wilmington, DE) and with the use of an RNA 6000 Nano Chip Kit with the Agilent 2100 Bioanalyzer (Agilent Technologies, Waldbronn, Germany). Amplification and Cy3 labeling the total RNA was performed using one-color Low Input Quick Amp Labeling Kit (Agilent Technologies) closely following the manufacturer's protocol. We used the Gene Expression Hybridization Kit (Agilent Technologies) for hybridization to SurePrint G3 Human Gene Expression 8x60K Microarrays (Agilent Technologies).

Data analysis for microarray

GeneSpring software GX 14.9.1 (Agilent Technologies) was used for data analysis (1.5-fold change and $P \leq 0.05$ cutoff). After importing the data, a standard baseline transformation to the median of all values was performed. After that a log transformation was performed and we computed the fold changes: log2(A/B) = log2(A)-log2(B). The following principle component analysis showed a homogenous component distribution. We excluded compromised array signals from further analysis. We defined an array spot as non-uniform if pixel noise of the feature exceeded the threshold or was above the saturation threshold. Genes that were regulated more than 1.5-fold were included in the subsequent analysis by using the paired Student's t-test and ($P<0.05$). Hierarchical cluster analysis of genes was generated using the GeneSpring GX 14.9.1 Hierarchical Clustering feature. We used Pearson's centered algorithm as the distance metric between gene entities and Ward's method as the criterion for linkage. Green represents low expression, grey represents moderate expression, and purple represents high expression. The Morpheus webtool was used to create the heat map (https://software.broadinstitute.org/morpheus/), and gene ontology analysis was performed using WebGestalt [5].

Quantitative real-time polymerase chain reaction

We used RNeasy Mini Kit (Qiagen, Hilden, Germany) for isolation of the RNA following the manufacture's protocol. We quantified the RNA concentration with the help of the NanoDrop 1000 system (PEQLAB, Erlangen, Germany). We performed cDNA synthesis using Maxima® reverse transcriptase (Fermentas, Waltham, MA) following the manufacturer's protocol.

We used Quantitative real-time polymerase chain reaction (qPCR) to quantify mRNA expression. **Table 1** shows the primer sequences and specific annealing temperatures. GAPDH was used for normalization of the expression levels. For our qPCR mix, 50 ng cDNA template was added to 12.5 µL KAPA-SYBR Fast Universal (PeqLab, Erlangen, Germany) and 0.5 µL of 20 pmol of each primer. We added water to a final volume of 25 µL. We used ΔΔCt method to compare relative expression after normalization.

Western blot

UD-SCC-5 cells were seeded in 6-well-plates (2.5×10^6 per culture dish). Cells were treated for 168 hours with 2xIC_{50} of afatinib and cisplatin. Furthermore, cells were costimulated with U0126 (25 µM). After the 168 hour treatment, cells were lysed in a buffer (20 mM Tris/HCl, pH 7.5, 150 mM NaCl, 1 mM Na_2EDTA, 1 mM EGTA, 1% Triton-X-100, 2.5 mM sodium pyrophosphate, 1 mM β-glycerophosphate, 1 mM Na_3VO_4, 1 µg/ml leupeptin, 1 mM PMSF). To precipitate insoluble membrane particles,

Table 1. Primer sequences and specific annealing temperature used in real-time quantitative PCR

Primer	Sequence	Annealing temperature [°C]
APOBEC2 forward	CCA GGC TGC TCT GAA GAA GC	60
APOBEC2 reverse	AGG CCT TGG ATT CAC CCT CT	60
APOBEC3B forward	GAC CCT TTG GTC CTT CGA C	60
APOBEC3B reverse	GCA CAG CCC CAG GAG AAG	60
APOBEC3C forward	GGA ACG AAA CTT GGC TGT GC	60
APOBEC3C reverse	CAG AAT CCA CCT GGT TTC GG	60
BRCA2 forward	AGA AGA AAC AAA GGC AAC GC	60
BRCA2 reverse	TGA GAA CAC GCA GAG GGA AC	60
GAPDH forward	GTG AAG GTC GGA GTC AAC GG	60
GAPDH reverse	TGA TGA CAA GCT TCC CGT TCT C	60
MLH1 forward	GTG CTG GCA ATC AAG GGA CCC	57
MLH1 reverse	CAC GGT TGA GGC ATT GGC TAG	57
MSH2 forward	CAG TAT ATT GGA GAA TGC CA	60
MSH2 reverse	AGG GCA TTT GTT TCA CC	60
MSH6 forward	AAC AAG GGG CTG GGT TAG	60
MSH6 reverse	CGT TGC ATT GCT CTC AGT ATT TC	60
MYC1 forward	TAT GTG GAG CGG CTT CTC G	60
MYC1 reverse	TGG GCT GTG AGG AGG TTT G	60
PARP1 forward	CCT GAT CCC CCA CGA CTT T	60
PARP1 reverse	GCA GGT TGT CAA GCA TTT C	60
POL_D1 forward	ATC CAG AAC TTC GAC CTT CCG	60
POL_D1 reverse	ACG GCA TTG AGC GTG TAG G	60
POL_i forward	AGT GTT GCC CAC ACC AAA TG	60
POL_i reverse	GTT GAA CCC CTA AAG GTT TGT CT	60
POL_K forward	TGG CAG TAT TTC ATT TCT TGT CA	60
POL_K reverse	TTT GAA TTA CAC ATT TTC TCT TGA GG	60
RAD51 forward	GCT GGG AAC TGC AAC TCA TCT	60
RAD51 reverse	GCA GCG CTC CTC TCT CCA GC	60
RAD52 forward	AGA CCT CTG ACA CAT TAG CCT TGA A	60
RAD52 reverse	AAG ATC CAG ATT TTG CTT GTG GTT	60
TET1 forward	ACC CCC TGT CAC CTG CTG AGG	57
TET1 reverse	GCG ATG GCC ACC CCA CCA AT	57
TET2 forward	TCA CAC CAG GTG CAC TTC TC	60
TET2 reverse	GGA TGG TTG TGT TTG TGC TG	60
TDG forward	GGC TAA TTG AGA GCG TGG AG	60
TDG reverse	GCA TGG CTT TCT TCT TCC TG	60
TOP1 forward	CGA AAA GAG GAA AAG GTT C	57
TOP1 reverse	GGG CTC AGC TTC ATG ACT TT	57
TOP2A forward	CTC CAC GAG AAA CAG AGC CA	57
TOP2A reverse	ACC GGT AGT GGA GGT GGA AG	57
XPC forward	ACA CCT ACT ACC TCT CAA ACC	60
XPC reverse	ATG GAC CAA TTC CTC ATC ATC TCG	60

lysates were centrifuged at 10,000 rpm for 15 min at 4°C. We used a Bradford assay to quantify protein concentrations. Equal amount of protein were loaded on the lanes in SDS-PAGE. All proteins were then transferred to a polyvinylidene difluoride (PVDF) membrane (Immobilon-P, Millipore, Germany). We blocked the membranes for one hour at room temperature with 5% nonfat dry milk in Tris-buffered saline containing 0.1% Tween 20 (TTBS). After a 12 h

incubation period with the primary antibodies shaking at 4°C, we added the secondary anti-IgG antibodies labeled with peroxidase in 5% nonfat dry milk in TTBS. The enhanced chemiluminescent (ECL) detection system with the imager SRX-101A (Konica Minolta, Langenhagen, Germany) was used to detected bands. Primary antibodies against the following antigens were used (dilution): p-stat3 Tyr705 (1:1000), p-Erk1/2 Thr202/Tyr204 (1:1000), p-p38 MAPK Thr180/Tyr182 (1:500), DNA polymerase iota (1:1000), APOBEC3B (1:1000), and Tubulin (1:5000). We used antibodies from US Biological (Marblehead, MA) and Cell Signaling Technology (Danvers, MA).

HPRT assay

Hypoxynthine phosphoribosyltransferase (HPRT) assay was used to measure changes in the mutation frequency as described previously [6]. First, mutant cleansing was performed by growing cells for 3 days in hypoxanthine-aminopterin-thymidine medium (HAT, Sigma, Germany). Following this, cells were grown 24 hours in hypoxanthine-thymidine medium (HT, Sigma, Germany). Cells were treated for 168 hours with cisplatin and afatinib only or costimulated with U0126. An untreated control was cocultivated, and, thereafter, cells were subcultured for 14 days. Cells (0.75/0.200 µl) were seeded in 96 wells, and 0.6 $\mu g/ml^{-1}$ of 6-TG (2-amino-6-mercaptopurine, Sigma, Germany) was added for negative selection, as only the cells containing the HPRT mutation can grow in 6-TG medium. 6-TG treated cells were incubated for 14 days; the medium was changed to DMEM, and cells were cultivated for another 14 days. Individual colonies were counted, and the number of colonies was normalized to the untreated control.

Statistical analysis

For statistical analysis we used GraphPad Prism 6.0 (Graph Pad Software Inc.). We tested the hypotheses with the help of one-way ANOVA. A $P<0.05$ was considered as statistical significant.

Results

To find a mechanism for the previously published result of an eightfold increase in mutation frequency of long term exposed cells to chemo- and targeted therapies [4] we first hypothesized that a change in gene expression happens early within the first seven days of exposion of the cells. We further hypothesized that this change would still be present in the long term exposed, resistant clones. We speculated that the actual mechanism of resistance to afatinib and to cisplatin would be distinct and by comparing similarities in afatinib and cisplatin treated cells a possible common mechanism in both could be identified.

To get an overview of the expression changes we first performed RNA expression analysis in a microarray. We compared cells treated with afatinib and cisplatin for 24 hours and 168 hours as well as the resistant clones. **Figure 1A** presents the clustered data. Differential gene expression revealed a total of 19,006 genes that were individually up- or downregulated. To break down this huge amount of changes we performed gene ontology analysis. **Figure 1B** indicates the top 10 positive and negative enrichment scores determined by gene ontology analysis for cells treated with afatinib for 168 hours. **Figure 1C** presents this analysis for cells treated with 168 hours of cisplatin. DNA replication is altered in cells treated with both afatinib and cisplatin. The polymerase delta 1 (POLD1) and polymerase delta 3 (POLD3) genes were downregulated in both. Alternation of DNA replication is also present at 24 hours of treatment (data not presented). Additionally, genes involved in repair mechanisms are downregulated in cisplatin-treated cells. These include postreplication, nonrecombinational, and nucleotide excision repair.

We speculated that finding a possible mechanism for the eightfold increase of mutation frequency within the 19,006 individually up-or downregulated genes would be laborsome. So instead, we focused our attention on an extensive literature search, looking for genes involved in DNA repair mechanisms or associated with genetic instability. We identified 20 possible candidates (**Figure 2**). Quantitative PCR revealed significant upregulation of RNA expression of APBOBEC3B, polymerase iota and XPC in both afatinib- and cisplatin-treated cells. Relative fold changes for afatinib and cisplatin were 1.58 and 3.12 for APOBEC3B, 2.45 and 2.10 for polymerase iota, and 2.72 and 1.83 for XPC. APOBEC2, APOBEC3C, and RAD52 were significantly upregulated in afatinib-stimulated cells but not in cisplatin. TDG was significantly downregulated in afatinib-treated cells.

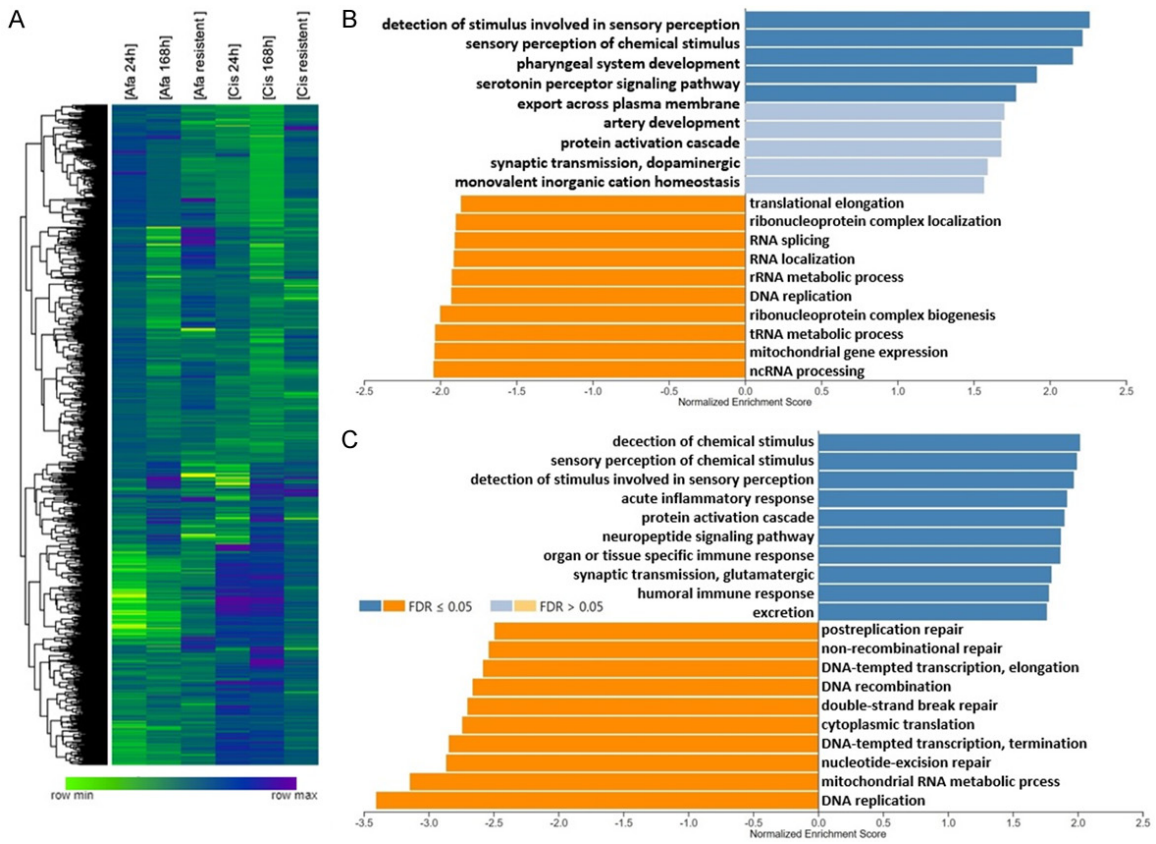

Figure 1. A: Clustered heat map indicating RNA expression of afatinib- and cisplatin-treated cells for 24 hours, 168 hours and 6 months (resistent). B: Gene ontology analysis indicating the top 10 positive and negative enriched gene sets in cells treated for 168 hours with afatinib. C: Gene ontology analysis revealing the top 10 positive and negative enriched gene sets in cells treated for 168 hours with cisplatin.

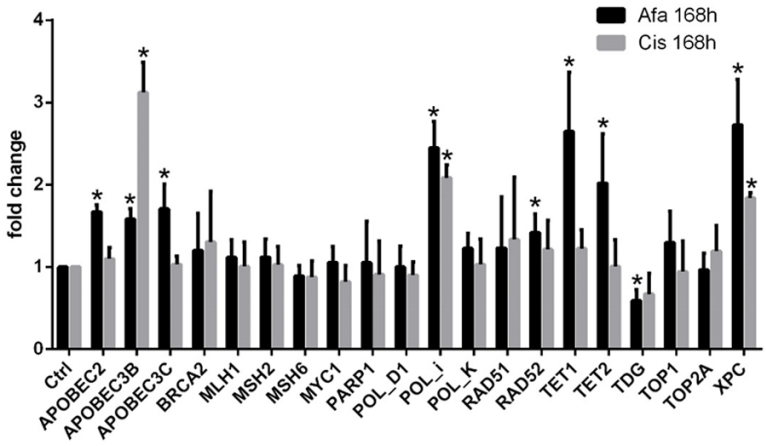

Figure 2. Fold change of RNA expression in qPCR of genes involved in DNA repair mechanisms. Cells were treated for 168 hours with afatinib and cisplatin, respectively. * indicates statistical significance.

Summarizing the results of RNA expression from **Figure 2**, in our view, the best candidates upregulated in both afatinib and cisplatin exposed cells are APOBEC3B, polymerase iota and XPC. For the further experiments, we focused our attention to APOBEC3B and polymerase iota.

Next we checked if upregulation of these two candidates would still be present on the protein level. Concordantly, the western blot revealed upregulation of A3B and polymerase iota in both afatinib- and cisplatin-treated clones (**Figure 3A**).

As previously published [4] we saw a switch to the ERK1/2 pathway in all 6 months long term exposed UD-SCC-5 clones. We postulate that this might represent a possible mechanism for regulation of A3B and polymerase iota. Indeed, the western blot in **Figure 3A** indicates concomitant upregulation

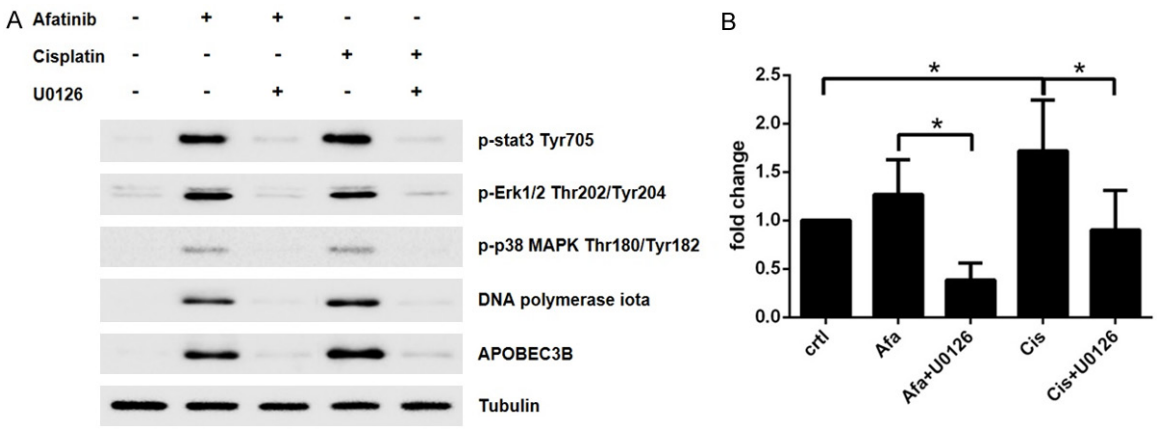

Figure 3. A: Western blot demonstrating MEK1/2-dependent upregulation of polymerase iota and APOBEC3B after 168 hours of stimulation with afatinib and cisplatin. Upregulation can be inhibited by costimulation with the MEK1/2 inhibitor U0126. B: Fold change in mutation frequency. * indicates statistical significance.

of ERK1/2, MEK1/2 and STAT3 even after 168 hours. To further solidify the role of MEK1/2 we used the MEK1/2 inhibitor U0126. In fact, costimulation of cells with afatinib or cisplatin and the MEK1/2 inhibitor U0126 led to downregulation of MEK1/2, ERK1/2, and STAT3 (**Figure 3A**). The western blot also revealed that afatinib and cisplatin cocultivation with U0126 results in downregulation of A3B and polymerase iota (**Figure 3A**) confirming our hypothesis.

Lastly, we speculated that the previously described increase in mutation frequency after six months [4] would already be detectable after 7 days and that costimulation of U016 by downregulation of MEK1/2 and concordant downregulation of A3B and polymerase iota would lead to a decrease in mutation frequency. To get evidence for this hypothesis, we determined the mutation frequency of afatinib, cisplatin, and the combination of afatinib+U0126 and cisplatin+U0126 costimulated cells by HRPT assay (**Figure 3B**). After 168 hours of incubation, cells treated with afatinib and cisplatin revealed a higher mutation frequency than the unstimulated control. Mean fold changes were 1.27 for afatinib and 1.72 for cisplatin. The result for cisplatin was statistically significant. The mean fold changes in mutation frequency in afatinib+U0126 and cisplatin+U0126 were 0.39 and 0.90, respectively. These results were significantly lower than those found in cells treated only with afatinib and cisplatin.

Discussion

Despite huge scientific effort, chemotherapy of most advanced tumors still rarely results in complete eradication. In most cases, tumors exhibit a varying degree of response and, ultimately, relapse with a more aggressive phenotype [1]. Tumor heterogeneity makes cancer a dynamic disease. There is evidence that bulk tumors consist of a diverse collection of cells with varying molecular signatures leading to different sensitivity to the therapy [7]. It is commonly assumed that selective pressure under therapy induces expansion of a preexisting nonsensitive clone, ultimately rendering the entire tumor resistant [7]. However, genomic instability may also be increased as a stress response during chemotherapy [8].

In our previous work, we generated resistant cell clones by long-term exposure over six months [4]. We used two cell lines and five targeted and chemotherapeutics (EGFR inhibitor afatinib, AKT inhibitor MK2206, MTOR/PI3K inhibitor BEZ235, PARP inhibitor olaparib, cisplatin). We found, on average, an eight-fold increase in mutation frequency. Interestingly, a targeted therapy such as afatinib also increased mutation frequency despite being an EGFR inhibitor and not affecting DNA as its primary mechanism of action. This may indicate that mutation frequency and, thus, genetic instability is dynamically regulated and could contribute to generation of resistant subclones.

In this work, we presented evidence that MEK1/2 is upregulating A3B and polymerase iota, leading to an increased mutation frequency after afatinib and cisplatin stimulation. In our microarray analysis, DNA replication was downregulated in both afatinib and cisplatin after 168 hours of treatment. This might also demonstrate a perturbation in DNA repair. We found subunits POLD1 and POLD3 downregulated in the array data in both afatinib- and cisplatin-treated cells. On the one hand, downregulation of POLD1 is associated with suppressed cell proliferation [9]. This may lead to a quiescent, less chemotherapeutic sensible state [10]. On the other hand, Tumini et al. indicated that downregulation of POLD1 and POLD3 give rise to genome instability hallmarks [11]. Czochor et al. present evidence that the oncogenic miRNA miR-155 downregulates all four subunits of the high-fidelity polymerase delta, promoting genomic instability [12].

In our work, the low-fidelity polymerase iota, which is part of the Y-Family polymerases, was upregulated on the RNA and the protein level. There is also evidence in the literature that this could potentially contribute to genetic instability. Y-Family polymerases exhibit a low fidelity and play an important role in error-prone translesion synthesis [13]. Hara et al. indicate that the high-fidelity polymerase delta is downregulated and the low-fidelity polymerases iota and epsilon are upregulated in prostate cancer cells during long-term exposure to the antiandrogen bicalutamide [14]. The authors speculate that this mechanism contributes to development of bicalutamide-resistant clones. Wojitaszek et al. found that inhibiting the small molecule JH-RE-06 disrupts mutagenetic translesion synthesis by preventing recruitment of polymerase ζ, leading to suppression of growth when coadministered with cisplatin in a melanoma xenograft model [15]. Perturbation of translesion polymerase activity by mutation or loss of expression can lead to accumulation of mutations in cells exposed to carcinogens [16].

The other possible mechanism we found for dynamically regulating the mutation frequency is A3B. There is a rising interest in uncovering the role of APOBEC in tumorigenesis. The APOBEC enzyme family was first discovered in HIV research. Sublethal APOBEC-induced mutagenesis of HIV virons has been linked to increased viron diversity and creation of drug-resistant variants [17]. A link between APOBEC in viral infection and cancer can be found in the human papilloma virus (HPV). HPV-positive HNSCC cells reveal a significantly higher fraction of a detectable APOBEC signature than those that are HPV-negative (98% versus 76%) [18]. APOBEC is also one of the most common mutational signatures, second only to those associated with age [19]. Overexpression of APOBEC is associated with increased mutational load [20]. While our results demonstrate an inducible rise in mutation frequency by chemotherapy, most studies propose APOBEC mutagenesis occurring late in the evolution of the primary tumor [21, 22]. Petljak et al. found APOBEC signatures fluctuating substantially over time with an episodic burst of mutation in 1,001 human cancer cell lines and 577 xerographs [23]. Roper et al. discovered that APOBEC mutagenesis correlated with mutational tumor heterogeneity in postmortem samples of primary and metastases of thoracic tumors [24]. In concordance with our hypothesis, Faltas et al. report an increased APOBEC-associated mutational load postchemotherapy in urothelial carcinoma [25]. Chou et al. demonstrated that afatinib-induced EGFR blockade attenuated b-Myb-related protein B and A3B expression [26]. The authors speculated that this would suppress mutagenesis. In our study, however, mutation frequency was elevated, though not statistically significantly, in afatinib-treated cells. Nonetheless, mutation frequency could be significantly reduced by costimulation with afatinib and the MEK inhibitor U0126.

In this work, we propose MEK1/2 as the mechanism for upregulating A3B and polymerase iota. In our previous work we found a switch to the ERK1/2 pathway as a commonality in the tested two cell lines long term exposed to five chemo- and targeted therapies [4]. In the literature Zou et al. report polymerase iota via EGFR ERK as a promotor of migration and invasion in breast cancer cells [27]. Zhenzi et al. promote ERK activation through polymerase iota [28], indicating a possible feedback loop. Although downstream consequences of APOBEC activity have been studied in viral infection and tumorigenesis, little is still known about the mechanisms regulating APOBEC expression [29]. In the literature, NF-κB, b-Myb-related protein B and MEK have been described. NF-κB activation via the protein kinase C (PKC) pathway was responsible for A3B expression in multiple can-

cer cell lines in a study by Maruyama et al. [30]. Similar to our findings, Rose et al. show a MEK dependent regulation of APOBEC3G [31].

Understanding mechanisms of the emergence of drug-resistant clones is essential in tumor therapy, and better knowledge could potentially lead to development of anti-evolutionary drugs [32]. When coadministered to standard therapy, these drugs could prevent or significantly delay formation of resistance. Treatment with U0126 may be beneficial in head and neck cancer in a clinical setting. Realistically, there will be multiple mechanisms and a vastly more complex regulatory network. Further research on this topic is needed.

Conclusion

In this work, we demonstrated that MEK1/2-induced upregulation of polymerase iota and APOBEC3B leads to an increased mutation frequency after 168 hours of afatinib and cisplatin stimulation. This may represent a plausible molecular mechanism of dynamically controlling genetic instability during chemotherapy in HNSCC cancer.

Disclosure of conflict of interest

None.

Address correspondence to: Dominik Schulz, Department of Internal Medicine II, Klinikum Rechts der Isar, Ismaninger Straße 22, Munich 81675, Germany. Tel: +0049-89-4140-2251; E-mail: Dominik.Schulz@mri.tum.de

References

[1] Xie K, Doles J, Hemann MT and Walker GC. Error-prone translesion synthesis mediates acquired chemoresistance. Proc Natl Acad Sci U S A 2010; 107: 20792-7.

[2] Dökümcü K and Farahani RM. Evolution of resistance in cancer: a cell cycle perspective. Front Oncol 2019; 9: 376.

[3] Rosenberg SM, Shee C, Frisch RL and Hastings PJ. Stress-induced mutation via DNA breaks in Escherichia coli: a molecular mechanism with implications for evolution and medicine. BioEssays 2012; 34: 885-892.

[4] Schulz D, Wirth M, Piontek G, Buchberger AM, Schlegel J, Reiter R, Multhoff G and Pickhard A. HNSCC cells resistant to EGFR pathway inhibitors are hypermutated and sensitive to DNA damaging substances. Am J Cancer Res 2016; 6: 1963-1975.

[5] Wang J, Vasaikar S, Shi Z, Greer M and Zhang B. WebGestalt 2017: a more comprehensive, powerful, flexible and interactive gene set enrichment analysis toolkit. Nucleic Acids Res 2017; 45: W130-W137.

[6] Johnson GE. Mammalian cell HPRT gene mutation assay: test methods. Genetic toxicology. Springer; 2012. pp. 55-67.

[7] Dagogo-Jack I and Shaw AT. Tumour heterogeneity and resistance to cancer therapies. Nat Rev Clin Oncol 2018; 15: 81-94.

[8] Fitzgerald DM, Hastings PJ and Rosenberg SM. Stress-induced mutagenesis: implications in cancer and drug resistance. Annu Rev Cancer Biol 2017; 1: 119-140.

[9] Song J, Hong P, Liu C, Zhang Y, Wang J and Wang P. Human POLD1 modulates cell cycle progression and DNA damage repair. BMC Biochem 2015; 16: 14.

[10] Chen W, Dong J, Haiech J, Kilhoffer MC and Zeniou M. Cancer stem cell quiescence and plasticity as major challenges in cancer therapy. Stem Cells Inter 2016; 2016: 1740936.

[11] Tumini E, Barroso S, Calero CP and Aguilera A. Roles of human POLD1 and POLD3 in genome stability. Sci Rep 2016; 6: 38873.

[12] Czochor JR, Sulkowski P and Glazer PM. miR-155 overexpression promotes genomic instability by reducing high-fidelity polymerase delta expression and activating error-prone DSB repair. Mol Cancer Res 2016; 14: 363-373.

[13] McCulloch SD and Kunkel TA. The fidelity of DNA synthesis by eukaryotic replicative and translesion synthesis polymerases. Cell Res 2008; 18: 148-161.

[14] Hara T, Kouno J, Nakamura K, Kusaka M and Yamaoka M. Possible role of adaptive mutation in resistance to antiandrogen in prostate cancer cells. Prostate 2005; 65: 268-275.

[15] Wojtaszek JL, Chatterjee N, Najeeb J, Ramos A, Lee M, Bian K, Xue JY, Fenton BA, Park H, Li D, Hemann MT, Hong J, Walker GC and Zhou P. A small molecule targeting mutagenic translesion synthesis improves chemotherapy. Cell 2019; 178: 152-159, e111.

[16] Makridakis N and Reichardt J. Translesion DNA polymerases and cancer. Front Genet 2012; 3: 174.

[17] Venkatesan S, Rosenthal R, Kanu N, McGranahan N, Bartek J, Quezada SA, Hare J, Harris RS and Swanton C. Perspective: APOBEC mutagenesis in drug resistance and immune escape in HIV and cancer evolution. Ann Oncol 2018; 29: 563-572.

[18] Cannataro VL, Gaffney SG, Sasaki T, Issaeva N, Grewal NKS, Grandis JR, Yarbrough WG, Burtness B, Anderson KS and Townsend JP. APOBEC-induced mutations and their cancer effect size in head and neck squamous cell carcinoma. Oncogene 2019; 38: 3475-3487.

[19] Alexandrov LB, Nik-Zainal S, Wedge DC, Aparicio SA, Behjati S, Biankin AV, Bignell GR, Bolli N, Borg A, Børresen-Dale AL, Boyault S, Burkhardt B, Butler AP, Caldas C, Davies HR, Desmedt C, Eils R, Eyfjörd JE, Foekens JA, Greaves M, Hosoda F, Hutter B, Ilicic T, Imbeaud S, Imielinski M, Jäger N, Jones DTW, Jones D, Knappskog S, Kool M, Lakhani SR, López-Otín C, Martin S, Munshi NC, Nakamura H, Northcott PA, Pajic M, Papaemmanuil E, Paradiso A, Pearson JV, Puente XS, Raine K, Ramakrishna M, Richardson AL, Richter J, Rosenstiel P, Schlesner M, Schumacher TN, Span PN, Teague JW, Totoki Y, Tutt ANJ, Valdés-Mas R, van Buuren MM, van't Veer L, Vincent-Salomon A, Waddell N, Yates LR, Zucman-Rossi J, Andrew Futreal P, McDermott U, Lichter P, Meyerson M, Grimmond SM, Siebert R, Campo E, Shibata T, Pfister SM, Campbell PJ and Stratton MR; Australian Pancreatic Cancer Genome Initiative; ICGC Breast Cancer Consortium; ICGC MMML-Seq Consortium; ICGC PedBrain. Signatures of mutational processes in human cancer. Nature 2013; 500: 415-421.

[20] Akre MK, Starrett GJ, Quist JS, Temiz NA, Carpenter MA, Tutt AN, Grigoriadis A and Harris RS. Mutation processes in 293-based clones overexpressing the DNA cytosine deaminase APOBEC3B. PLoS One 2016; 11: e0155391.

[21] Jamal-Hanjani M, Wilson GA, McGranahan N, Birkbak NJ, Watkins TBK, Veeriah S, Shafi S, Johnson DH, Mitter R, Rosenthal R, Salm M, Horswell S, Escudero M, Matthews N, Rowan A, Chambers T, Moore DA, Turajlic S, Xu H, Lee SM, Forster MD, Ahmad T, Hiley CT, Abbosh C, Falzon M, Borg E, Marafioti T, Lawrence D, Hayward M, Kolvekar S, Panagiotopoulos N, Janes SM, Thakrar R, Ahmed A, Blackhall F, Summers Y, Shah R, Joseph L, Quinn AM, Crosbie PA, Naidu B, Middleton G, Langman G, Trotter S, Nicolson M, Remmen H, Kerr K, Chetty M, Gomersall L, Fennell DA, Nakas A, Rathinam S, Anand G, Khan S, Russell P, Ezhil V, Ismail B, Irvin-Sellers M, Prakash V, Lester JF, Kornaszewska M, Attanoos R, Adams H, Davies H, Dentro S, Taniere P, O'Sullivan B, Lowe HL, Hartley JA, Iles N, Bell H, Ngai Y, Shaw JA, Herrero J, Szallasi Z, Schwarz RF, Stewart A, Quezada SA, Le Quesne J, Van Loo P, Dive C, Hackshaw A and Swanton C; TRACERx Consortium. Tracking the evolution of non-small-cell lung cancer. N Engl J Med 2017; 376: 2109-2121.

[22] de Bruin EC, McGranahan N, Mitter R, Salm M, Wedge DC, Yates L, Jamal-Hanjani M, Shafi S, Murugaesu N, Rowan AJ, Gronroos E, Muhammad MA, Horswell S, Gerlinger M, Varela I, Jones D, Marshall J, Voet T, Van Loo P, Rassl DM, Rintoul RC, Janes SM, Lee SM, Forster M, Ahmad T, Lawrence D, Falzon M, Capitanio A, Harkins TT, Lee CC, Tom W, Teefe E, Chen SC, Begum S, Rabinowitz A, Phillimore B, Spencer-Dene B, Stamp G, Szallasi Z, Matthews N, Stewart A, Campbell P and Swanton C. Spatial and temporal diversity in genomic instability processes defines lung cancer evolution. Science 2014; 346: 251-256.

[23] Petljak M, Alexandrov LB, Brammeld JS, Price S, Wedge DC, Grossmann S, Dawson KJ, Ju YS, Iorio F and Tubio JM. Characterizing mutational signatures in human cancer cell lines reveals episodic APOBEC mutagenesis. Cell 2019; 176: 1282-1294, e1220.

[24] Roper N, Gao S, Maity TK, Banday AR, Zhang X, Venugopalan A, Cultraro CM, Patidar R, Sindiri S, Brown AL, Goncearenco A, Panchenko AR, Biswas R, Thomas A, Rajan A, Carter CA, Kleiner DE, Hewitt SM, Khan J, Prokunina-Olsson L and Guha U. APOBEC mutagenesis and copy-number alterations are drivers of proteogenomic tumor evolution and heterogeneity in metastatic thoracic tumors. Cell Rep 2019; 26: 2651-2666, e2656.

[25] Faltas BM, Prandi D, Tagawa ST, Molina AM, Nanus DM, Sternberg C, Rosenberg J, Mosquera JM, Robinson B, Elemento O, Sboner A, Beltran H, Demichelis F and Rubin MA. Clonal evolution of chemotherapy-resistant urothelial carcinoma. Nat Genet 2016; 48: 1490-1499.

[26] Chou WC, Chen WT, Hsiung CN, Hu LY, Yu JC, Hsu HM and Shen CY. B-Myb induces APOBEC3B expression leading to somatic mutation in multiple cancers. Sci Rep 2017; 7: 44089.

[27] Zou S, Xu Y, Chen X, He C, Gao A, Zhou J and Chen Y. DNA polymerase iota (Pol ι) promotes the migration and invasion of breast cancer cell via EGFR-ERK-mediated epithelial to mesenchymal transition. Cancer Biomark 2019; 24: 363-370.

[28] Su Z, Gao A, Li X, Zou S, He C, Wu J, Ding WQ and Zhou J. DNA polymerase iota promotes esophageal squamous cell carcinoma proliferation through Erk-OGT-induced G6PD overactivation. Front Oncol 2021; 11: 706337.

[29] Covino DA, Gauzzi MC and Fantuzzi L. Understanding the regulation of APOBEC3 expression: current evidence and much to learn. J Leukoc Biol 2018; 103: 433-444.

[30] Maruyama W, Shirakawa K, Matsui H, Matsumoto T, Yamazaki H, Sarca AD, Kazuma Y, Kobayashi M, Shindo K and Takaori-Kondo A. Classical NF-κB pathway is responsible

for APOBEC3B expression in cancer cells. Biochem Biophys Res Commun 2016; 478: 1466-1471.

[31] Rose KM, Marin M, Kozak SL and Kabat D. Transcriptional regulation of APOBEC3G, a cytidine deaminase that hypermutates human immunodeficiency virus. J Biol Chem 2004; 279: 41744-41749.

[32] Gatenby R and Whelan C. Cancer treatment innovators discover Charles Darwin. Evol Med Public Health 2019; 2019: 108-110.